Nanotechnology Perceptions
ISSN 1660-6795
www.nano-*ntp.com*

PEDOT Composites With Nanocellulose Enhancement As High-Performance, Sustainable Supercapacitor Electrodes

Bhanu Gupta

Research Scholar, Department of Chemistry, Deenbandhu Chhotu Ram University of Science and Technology, Murthal, Haryana-131039, India.
Email: 19001952001bhanu@dcrustm.org

Lightweight, adaptable, and efficient energy storage systems are required due to the growing demand for portable electronics and renewable energy applications. In this work, nanocellulose (NC) derived from sugarcane bagasse and poly(3,4-ethylenedioxythiophene) (PEDOT) are combined to create a new composite material for high-performance supercapacitor electrodes. A number of chemical procedures, such as delignification, alkali treatment, and acid hydrolysis, were used to remove the nanocellulose. Ferric chloride ($FeCl_3$) was used in oxidative polymerization to create PEDOT. In situ polymerization produced the resulting PEDOT/NC composites, which were then examined using electrochemical, FTIR, XRD, FESEM, and TGA techniques. SEM images revealed a fibrillated, porous shape that was ideal for storing charge, while FTIR and XRD confirmed the successful integration and preservation of structural integrity. The composites had better thermal stability, according to a thermal study. A significant rise in specific capacitance was detected by cyclic voltammetry, which gauges electrochemical performance. The pristine PEDOT (X4, 102 F/g) was greatly outperformed by the PEDOT/NC composite PX5, which achieved a high of 660 F/g. These findings suggest that NC and PEDOT can cooperate, which makes the composite a good choice for next-generation, environmentally friendly supercapacitors.

Keywords: conducting polymers (CPs), Nanocellulose (NC), Poly(3,4-ethylenedioxythiophene) (PEDOT).

1. Introduction

The need for high power density, light weight, and flexible energy storage devices is growing urgently as a result of the dearth of renewable energy sources and the pervasive use of portable electronic gadgets. The development of supercapacitors has accelerated and entered the "speed-up era" due to the emergence of improved carbon materials, which offer benefits such as high surface area, high electrical conductivity, high mechanical qualities, and more. It is commonly known that in the upcoming years, supercapacitors will take the place of traditional batteries and capacitors. In addition, supercapacitors have a higher energy density than regular capacitors, which makes them capable of faster charging and more energy storage.

Consequently, a great deal of interest has grown in the area of energy storage in supercapacitors and supercapacitor-battery hybrid devices, with research concentrating on the creation of new materials that could improve the efficiency of devices[1][2].

The electrochemical performance of a supercapacitor can be enhanced by altering the electrode materials, as the electrode material's performance determines the supercapacitor's total performance. Because of their high conductivity and inexpensive synthesis costs, conducting polymers (CPs) are being used as the active material in supercapacitors. Conjugated bonds along the polymer backbone give conducting polymers their conductive properties. The most often researched polymers for usage in supercapacitor devices are polypyrrole, polyaniline, and polythiophene derivatives. Out of all the conducting polymers, poly (3,4-ethylenedioxythiophene) (PEDOT) has attracted a lot of attention as a supercapacitor electrode material because of its superior stability in the oxidized state, strong thermal stability, and environmental steadiness. The alternate double (π) and single (σ) bonds that run along the CPs chains make up the conjugated system, which is the structure of a CP. Nonetheless, in comparison to semiconductors, the majority of CPs continues to have limited electrical conductivity. Consequently, in order to improve the electrical conductivity, doping is necessary[3][4].

Nanocellulose (NC) has been extensively studied and characterized in recent years. Generally, NC, which has a structure resembling a rod, needle, or ribbon, has a few intriguing qualities, including low density, high surface area, renewability, and great strength[5][6][7]. The most prevalent natural polymeric substance on the planet is cellulose, which is found in bacteria, fungus, algae, plants, and marine life (tunicates), among other sources. Furthermore, because of its exceptional specific strength and modulus, low coefficient of thermal expansion, low density, high aspect ratio, biodegradability, renewability, and biocompatibility, Nano-cellulose which is isolated from cellulosic sources at the nanoscale has attracted a lot of attention from both the academic and industrial sectors. Not only is NC widely accessible, but it may also be environmentally safe and derived from a variety of sources by acid hydrolysis[8][9].

It is well known that NCC has a lower electrical conductivity than other carbon-based materials. On the other hand, NCC may be altered with PEDOT to provide remarkable mechanical strength and improved electrical conductivity. In this study, a flexible and electrically conducting composite material was created by using nanocellulose as the matrix and PEDOT as the conducting component[10][11][12][13].

2. Experimental

2.1 Materials

All of the reagents used were of analytical grade, including EDOT (Sigma Aldrich), Ferric Chloride (CDH), Sulfuric Acid with 98% Assay supplied by (Qualikems), Methanol bought from Rankem, and Sodium Chlorite and Sulfite (Sigma Aldrich and Sigma Aldrich, respectively). All other compounds, including EDOT, were used just as supplied, requiring no further purification. Throughout the whole procedure, double-distilled water was utilized.

2.2 Preparation of PEDOT

Poly(3,4-ethylenedioxythiophene) (PEDOT) was produced by chemical oxidative polymerization using ferric chloride ($FeCl_3$) as the oxidizing agent. The 3,4-ethylenedioxythiophene (EDOT) monomer was first dissolved in Double Distilled water while being continuously stirred. A different weight % of $FeCl_3$ was then gradually added to the solution to initiate the polymerization process. The reaction mixture was constantly agitated for 12 hours at room temperature in order to ensure complete monomer conversion. During the polymerization process, PEDOT, a dark blue solid, precipitated. The final polymer was filtered out and then cleaned with methanol, deionized water, and acetone in order to remove any remaining oxidant. The PEDOT was vacuum-dried at 60 °C for 24 hours after purification.

Table 1. Sample preparation of PEDOT at different concentration of $FeCl_3$

Sr. No.	Sample code	EDOT: $FeCl_3$ (w/w ratio)
1.	X1	1:0.5
2.	X2	1:1
3.	X3	1:1.5
4.	X4	1:2
5.	X5	1:2.5
6.	X6	1:3.0

2.3 Synthesis of Nanocellulose

Nanocellulose was made from sugarcane bagasse using three main phases in a sequential chemical treatment process. Initially, the bagasse was treated with an aqueous sodium chlorite solution at 45°C for five hours in order to remove the lignin. A further treatment with aqueous sodium sulfite under identical circumstances resulted in the production of holocellulose. The second stage was alkalinely extracting hemicellulose using an aqueous sodium hydroxide solution at 45°C for five hours in order to produce purified cellulose. Following five hours of treatment at 45°C with diluted sulfuric acid, the cellulose was subjected to controlled acid hydrolysis, and centrifugation was used to extract the nanocellulose crystals. This systematic procedure effectively separated the lignocellulosic components, producing usable and further defined nanocellulose.

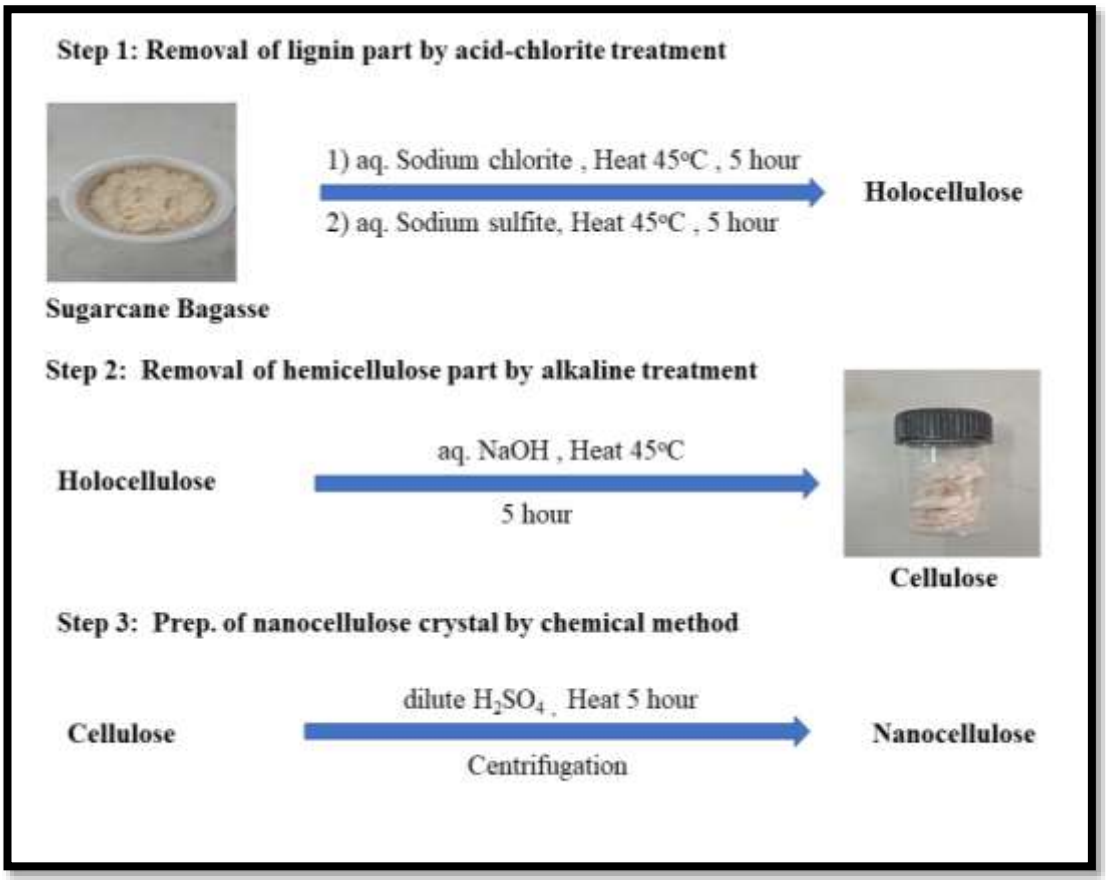

Figure 1. Preparation of nanocrystalline cellulose from sugarcane bagasse

2.4 composite formation

In this study, ferric chloride ($FeCl_3$) and PEDOT were mixed into a conductive composite made from nanocellulose using a method called in situ oxidative polymerization. In order to produce a homogeneous colloidal suspension, nanocellulose was first ultrasonically dissolved in deionized water. The EDOT monomer was dissolved by this NC solution. $FeCl_3$ was then added to the reaction mixture dropwise at a molar weight percentage of about 1:2 of EDOT. By letting the polymerization reaction run for 12 hours while being constantly stirred, PEDOT chains were completely formed inside the nanocellulose network. The resulting dark blue precipitate was filtered, and then it was cleaned with ethanol and deionized water one after the other until the pH of the filtrate was neutral. It was then vacuum-dried at 50°C to yield a porous nanocellulose-PEDOT composite.

Table 2. COMPOSITE of PEDOT/NC at different concentration of NC

Sr. No.	Sample code	EDOT:NC (w/w ratio)
1.	PX1	99.5:0.5
2.	PX2	99.0:1
3.	PX3	98.5:1.5
4.	PX4	98:2
5.	PX5	97.5:2.5
6.	PX6	97:3

3. Characterization Techniques

3.1 Infrared spectroscopy using Fourier transforms (FT-IR)

The functional groups of the PEDOT nanoparticles were identified using an FTIR spectrometer (Thermo Nicolet, Nexus670). The KBr pellet method was used to prepare the samples, and KBr served as the background material. The spectrometer was run in absorption mode, and 32 scans with a resolution of 4 cm^{-1} encompassing the 400–4000 cm^{-1} wavenumber range were used to generate the spectra.

3.2 Derivative thermal gravimetric (DTG) and thermal gravimetric analysis (TGA)

Using a thermogravimetric analyzer (PerkinElmer, TGA7), the thermal behavior of the nanoparticles was examined. An aluminum pan was filled with samples weighing five to ten milligrams. The mass change was measured under nitrogen flow between 30 and 900◦C at a heating rate of 10◦Cmin^{-1}.

3.3 X-ray Diffraction (XRD) Spectroscopy

The crystalline structure of the nanoparticles was ascertained using a wide-angle X-ray diffractometer (Bruker AXS, D8Advance). 40 kV/30 mA was the operating voltage for the Cu Kα radiation source. Using a K-beta filter, the interference peak was removed. In addition to a 0.3 mm receiving slit, a 0.5◦ scattering and divergence slit were employed. After the nanoparticles were placed on a sample holder, a continuous measurement was conducted. With a scan speed of 1 min−1 and a scan step of 0.02 ◦, the experiment was conducted by tracking the diffraction pattern that appeared in the 2θ range of 10◦ to 80◦.

3.4 Scanning electron microscopy with field emission (FESEM)

A field emission scanning electron microscope (TESCAN MIRA3 FEG-SEM) running at 18 kV was used to examine the surface morphology of clean PEDOT and its composites. All of the trials were conducted using powder.

3.5 Electrochemical Characterization

A three-electrode system with a reference electrode of silver-silver chloride and a counter electrode of platinum was used to measure the electrochemical performance of the composites using an electrochemical workstation (PGSTAT 204 Autolab, Netherlands) equipped with a FRA 32M module and NOVA 1.11 software. For every manufactured electrode material, cyclic voltage monitoring (CV), electrochemical impedance spectroscopy (EIS), and galvanostatic charge discharge (GCD) were monitored during these studies[14][10][15].

4. Result and Discussion

4.1 FTIR analysis

Fourier-transform infrared (FTIR) spectroscopy was employed to investigate the chemical structure and functional group modifications of pristine PEDOT and doped PEDOT. The spectra revealed characteristic absorption bands corresponding to various vibrational modes in both samples. A broad peak observed around 3435 cm^{-1} is attributed to O–H stretching vibrations, indicating the presence of moisture or hydroxyl groups. In the fingerprint region, notable shifts and changes in intensity are observed upon doping. The undoped PEDOT exhibited absorption bands at 1617, 1561, and 1417 cm^{-1}, corresponding to C=C stretching vibrations of the thiophene ring and asymmetric/symmetric stretching of the sulfonate groups. In the doped PEDOT(PEDOT/NC), slight shifts in these bands (e.g., from 1617 to 1641 cm^{-1}) indicate interactions between the dopant and the polymer backbone. The peaks at 1343 and 1205 cm^{-1} are associated with C–C inter-ring stretching and C–O–C ether vibrations, respectively. The overall reduction in transmittance and spectral shifts in the doped PEDOT confirm successful doping and suggest structural reorganization or enhanced conjugation in the polymer matrix[16][17].

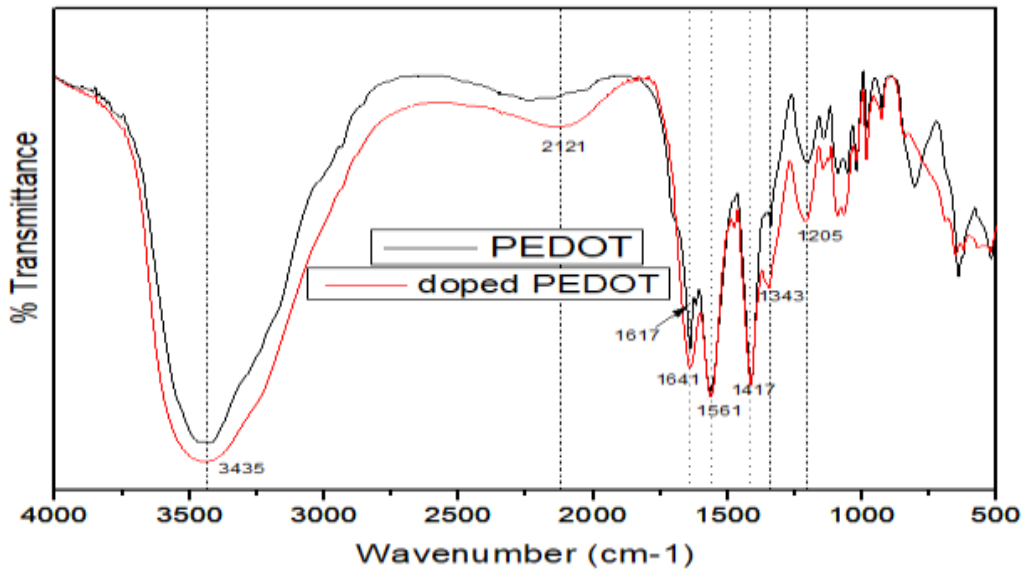

Figure 2. (a) FTIR of PEDOT (X4) and doped PEDOT (PX4).

During the isolation process, the chemical structures of sugarcane bagasse, cellulose, and nanocellulose were examined using Fourier-transform infrared (FTIR) spectroscopy. A broad absorption band at about 3448 cm^{-1} can be seen in the raw sugarcane bagasse spectrum (black curve), which is ascribed to absorbed moisture and O–H stretching vibrations of hydroxyl groups. The C=O stretching of hemicellulose and lignin is represented by the peaks seen around 1640 cm^{-1} and 1560 cm^{-1}, respectively. The prominent peak at 1019 cm^{-1} is indicative of the C–O stretching vibrations of cellulose and hemicellulose, whereas the band around 1420 cm^{-1} is attributed to CH_2 bending. Following the alkaline and bleaching processes to produce cellulose (red curve), lignin and hemicellulose are effectively removed as evidenced by the sharp decline in peak intensity around 1640 cm^{-1} and 1560 cm^{-1}. High cellulose purity is confirmed by the further band reduction and widening shown in the nanocellulose sample (green curve), particularly the elimination of the lignin-associated peaks. Furthermore, the β-glycosidic bonds of cellulose are responsible for the band at 926 cm^{-1} that is clearly visible in nanocellulose, suggesting that the cellulose backbone structure has been preserved[8]. All things considered, the comparative FTIR analysis validates the effective conversion of sugarcane bagasse into pure nanocellulose and the gradual elimination of non-cellulosic components.

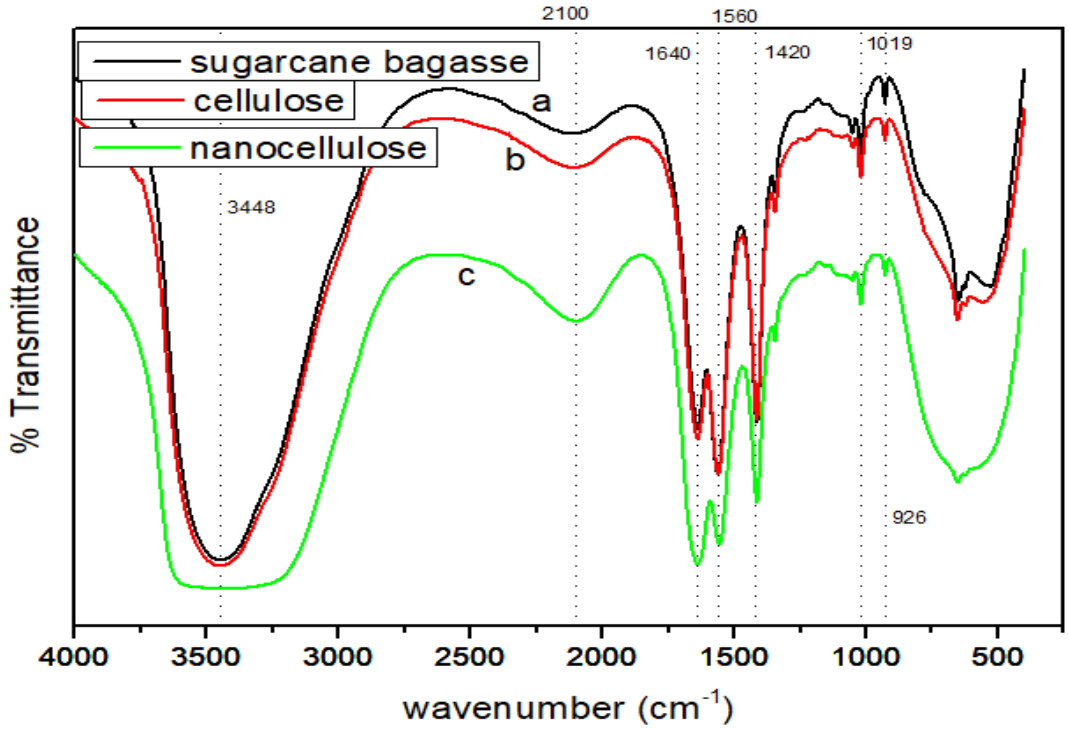

Figure 2. (b) FTIR of sugarcane bagasse, cellulose and nanocellulose.

4.2 XRD

The X-ray diffraction pattern of NC is seen in Fig. 4. This analysis revealed a high intensity peak at 2θ = 22.8°, which was caused by diffraction from the (200) plane. Additional double peak signals were seen at = 14.8° and 16.5°, respectively, as a result of reflections from (110) and (110) diffraction (Fig. 4). The XRD traces showed a clear retention of the cellulose crystallites and an enhancement of peak intensity at 2θ = 14.8°, 16.5°, 22.8°, and 34.5°. The dried NC was found to be almost 90% crystalline. The higher the value of the specified index, the more crystalline the test material is and the more ordered its structure is[4][18].

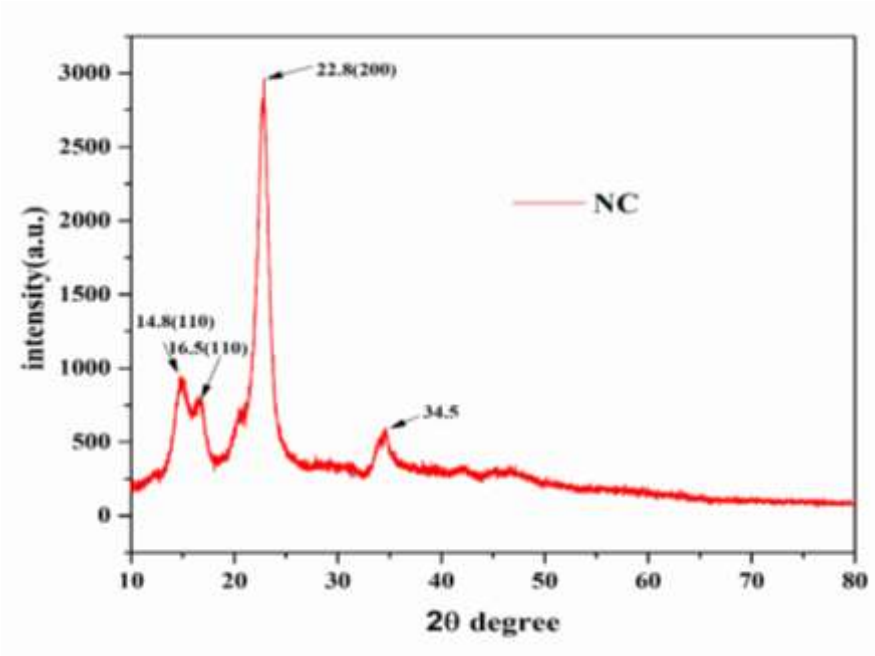

The NC sample's crystalline structure—likely nanocellulose—is shown by the X-ray diffraction (XRD) pattern. A semi-crystalline cellulose I structure is indicated by the diffraction peaks at 2θ values of 14.8° and 16.5°, which are attributed to the (110) planes, and a strong peak at 22.8°, which corresponds to the (200) plane. The 34.5° peak might indicate extra phases or trace amounts of crystalline impurities. A considerable amount of crystallinity is reflected in the (200) peak's high intensity. All things considered, this pattern demonstrates that the NC sample has an ordered cellulose lattice with a few amorphous areas, which is typical of nanocellulose materials made from natural sources.

4.3 SEM

As seen in Figure, the untreated cellulose biomass (left picture) displayed large, smooth, plate-like formations with relatively intact surfaces. This observation suggests that there has been minimal disruption to the original cellulose matrix. However, the partially treated sample (middle picture) displayed a variety of morphologies, with larger remnant pieces dispersed throughout tangled fiber networks. This observation indicates defibrillation and partial

breakage of cellulose bundles. The fully processed nanocellulose (right picture) exhibited a highly fibrillated and porous structure, consisting of nanoscale fibrils. This result confirms that the cellulose has significantly broken down into either individual nanofibers or loosely aggregated nanofibers. It is clear from these slow morphological changes how effectively the specified treatment transforms cellulose biomass into nanocellulose[19].

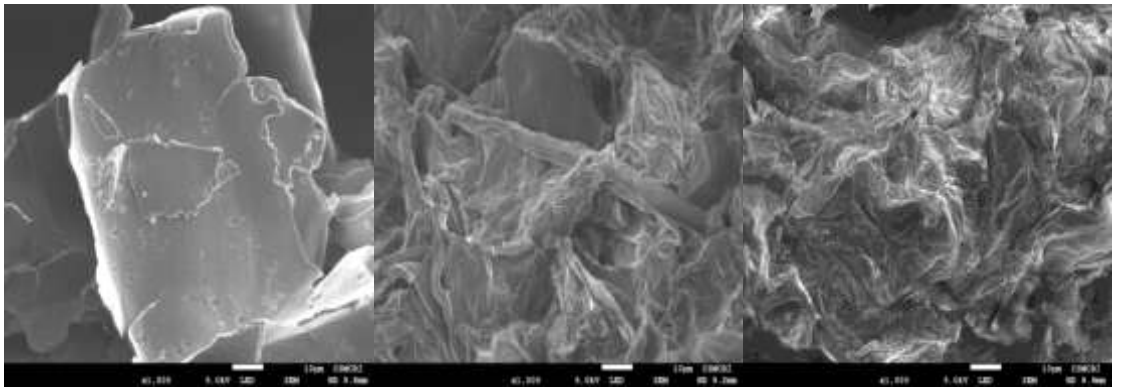

4.4 TGA

This thermogravimetric analysis (TGA) figure plots the mass loss (%) for NC (blue), cellulose (red), and sugarcane bagasse (black) against temperature. Each sample exhibits a stable initial phase up to about 250 °C, followed by a notable breakdown between roughly 250 and 400 °C. Cellulose decomposes more quickly and leaves the least amount of residue, whereas sugarcane bagasse has more residual mass and higher thermal stability. The intermediate behavior of NC indicates a partial removal of non-cellulosic components[20][3].

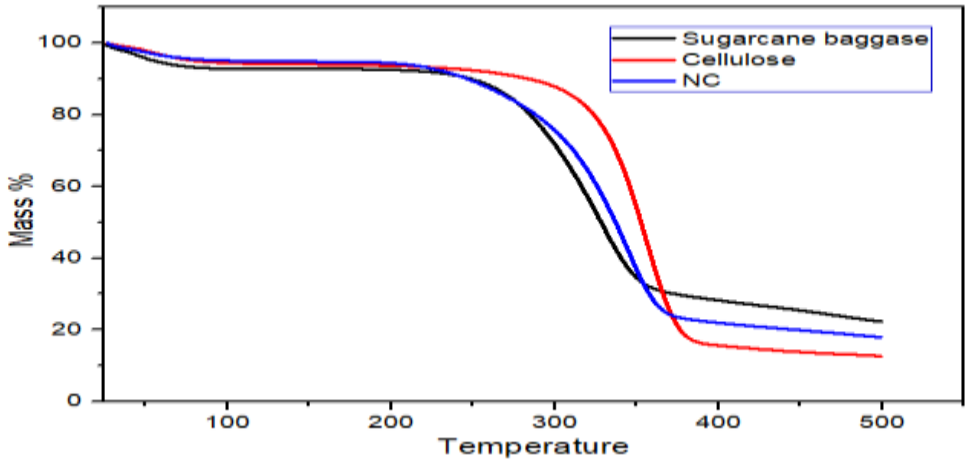

4.5 ELECTROCHEMICAL APPLICATIONS

4.5.1 Cyclic voltametry

Cyclic voltammetry (CV) was used to evaluate the electrochemical behavior of two sets of electrode materials, X1 to X6 and nanocellulose doped PEDOT PX1 to PX6, with an active mass loading of roughly 1 mg each. The X-series CV curves (X1–X6), which primarily have rectangular geometries and relatively low current densities, illustrate electric double-layer capacitive (EDLC) behavior. While X1 and X2 have the least amount of current response, indicating little electrochemical activity, X4, which has the largest enclosed area, indicates the group's highest specific capacitance (102 F/g). On the other hand, the PX-series (PX1–PX6) exhibits notably higher larger loop areas and enhanced specific capacitance PX5 (660 F/g). The presence of faradaic redox reactions, which are suggestive of pseudocapacitive behavior, is indicated by the wider and distorted forms of these curves. This enhanced reaction could be caused by a more porous structure, improved electrical conductivity, or the presence of redox-active surface functions. Overall, under NC mass loading conditions, the PX-series materials—especially PX5—perform better electrochemically than the X-series, making them more desirable choices for high-performance energy storage applications[21][5].

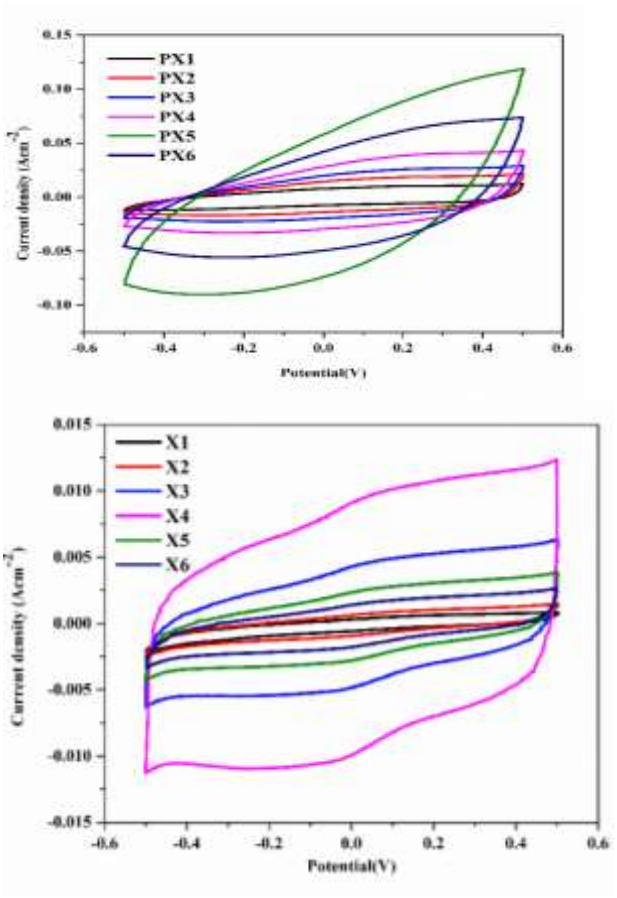

Table 3. Specific capacitance of PEDOT at different concentration of $FeCl_3$

Sr. No.	Sample code	Specific capacitance(F/g)
1.	X1	21
2.	X2	48
3.	X3	73
4.	X4	102
5.	X5	65
6.	X6	54

Table 4. Specific capacitance of Composite

Sr. No.	Sample code	Specific capacitance(F/g)
1.	PX1	285
2.	PX2	330
3.	PX3	380
4.	PX4	460
5.	PX5	660
6.	PX6	510

5. CONCLUSION

This work effectively synthesizes and integrates poly(3,4-ethylenedioxythiophene) (PEDOT) with nanocellulose (NC) derived from sugarcane bagasse to create advanced composite materials for supercapacitor electrodes. Intact crystalline structure and the removal of non-cellulosic biomass were revealed by FTIR and XRD tests, which confirmed that the extensive chemical treatments effectively separated high-purity nanocellulose. According to SEM, the in situ oxidative polymerization process evenly integrated PEDOT into the NC scaffold, resulting in a composite with a highly fibrillated, porous morphology. Thermal studies show that the resultant composites retain excellent thermal stability, indicating that they could be appropriate for demanding energy storage applications. Specifically, electrochemical measurements showed that the PEDOT/NC composites had significantly increased specific capacitance, reaching 660 F/g for PX5, which is significantly higher than the performance of pristine PEDOT (102 F/g).

REFERENCES

[1] P. Rani, R.S. Malik, Electromagnetic interference shielding behavior of polypyrrole-impregnated poly(ether imide)/sulfonated poly(ether ether ketone) composites, Mater. Chem. Phys. 307 (2023) 128187. https://doi.org/10.1016/j.matchemphys.2023.128187.

[2] D. Mohanadas, M. Amirul, A. Mohd, N. Hawa, N. Azman, Facile synthesis of PEDOT - rGO / HKUST - 1 for high performance symmetrical supercapacitor device, Sci. Rep. (2021) 1–14. https://doi.org/10.1038/s41598-021-91100-x.

[3] Z. Wang, D.O. Carlsson, P. Tammela, K. Hua, P. Zhang, L. Nyholm, M. Strømme, Surface Modified Nanocellulose Fibers Yield Conducting Polymer-Based Flexible Supercapacitors

with Enhanced Capacitances, ACS Nano 9 (2015) 7563–7571. https://doi.org/10.1021/acsnano.5b02846.
[4] R. Ravit, J. Abdullah, I. Ahmad, Y. Sulaiman, nanocrystalline cellulose (PEDOT / NCC) fi lm for supercapacitor, Carbohydr. Polym. 203 (2019) 128–138. https://doi.org/10.1016/j.carbpol.2018.09.043.
[5] R. Arora, S.P. Nehra, S. Lata, In-situ composited g-C3N4/polypyrrole nanomaterial applied as energy-storing electrode with ameliorated super-capacitive performance, Environ. Sci. Pollut. Res. 30 (2023) 98589–98600. https://doi.org/10.1007/s11356-022-21777-8.
[6] Q. Meng, K. Cai, Y. Chen, L. Chen, Nano Energy Research progress on conducting polymer based supercapacitor electrode materials, Nano Energy 36 (2017) 268–285. https://doi.org/10.1016/j.nanoen.2017.04.040.
[7] I. Shown, A. Ganguly, L.C. Chen, K.H. Chen, Conducting polymer-based flexible supercapacitor, Energy Sci. Eng. 3 (2015) 2–26. https://doi.org/10.1002/ese3.50.
[8] G.A. Tafete, M.K. Abera, G. Thothadri, Review on nanocellulose-based materials for supercapacitors applications, J. Energy Storage 48 (2022) 103938. https://doi.org/10.1016/j.est.2021.103938.
[9] R. Brooke, M. Lay, K. Jain, H. Francon, M.G. Say, D. Belaineh, X. Wang, K.M.O. Håkansson, L. Wågberg, I. Engquist, J. Edberg, M. Berggren, Nanocellulose and PEDOT:PSS composites and their applications, Polym. Rev. 63 (2023) 437–477. https://doi.org/10.1080/15583724.2022.2106491.
[10] R. Ravit, J. Abdullah, I. Ahmad, Y. Sulaiman, Electrochemical performance of poly(3, 4-ethylenedioxythipohene)/nanocrystalline cellulose (PEDOT/NCC) film for supercapacitor, Carbohydr. Polym. 203 (2019) 128–138. https://doi.org/10.1016/j.carbpol.2018.09.043.
[11] M. Lay, M.G. Say, I. Engquist, Direct Ink Writing of Nanocellulose and PEDOT:PSS for Flexible Electronic Patterned and Supercapacitor Papers, Adv. Mater. Technol. 8 (2023) 1–11. https://doi.org/10.1002/admt.202300652.
[12] D. Zhao, Q. Zhang, W. Chen, X. Yi, S. Liu, Q. Wang, Y. Liu, J. Li, X. Li, H. Yu, Highly Flexible and Conductive Cellulose-Mediated PEDOT:PSS/MWCNT Composite Films for Supercapacitor Electrodes, ACS Appl. Mater. Interfaces 9 (2017) 13213–13222. https://doi.org/10.1021/acsami.7b01852.
[13] T.F. Iorfa, K.F. Iorfa, A.A. Mcasule, M.A. Akaayar, Extraction And Characterization of Nanocellulose From Rice Husk, 7 (2020) 3–4.
[14] P. Damlin, C. Kvarnström, A. Ivaska, Electrochemical synthesis and in situ spectroelectrochemical characterization of poly(3,4-ethylenedioxythiophene) (PEDOT) in room temperature ionic liquids, J. Electroanal. Chem. 570 (2004) 113–122. https://doi.org/10.1016/j.jelechem.2004.03.023.
[15] A. Yang, J.T. Lin, C. Li, Electroactive and Sustainable Cu-MOF / PEDOT Composite Electrocatalysts for Multiple Redox Mediators and for High- Performance Dye-Sensitized Solar Cells, (2021). https://doi.org/10.1021/acsami.0c21542.
[16] B. Li, H. Lopez-Beltran, C. Siu, K.H. Skorenko, H. Zhou, W.E. Bernier, M.S. Whittingham, W.E. Jones, Vaper Phase Polymerized PEDOT/Cellulose Paper Composite for Flexible Solid-State Supercapacitor, ACS Appl. Energy Mater. 3 (2020) 1559–1568. https://doi.org/10.1021/acsaem.9b02044.
[17] K. Lota, V. Khomenko, E. Frackowiak, Capacitance properties of poly (3 , 4-ethylenedioxythiophene)/ carbon nanotubes composites, 65 (2004) 295–301. https://doi.org/10.1016/j.jpcs.2003.10.051.
[18] G.A. Snook, P. Kao, A.S. Best, Conducting-polymer-based supercapacitor devices and electrodes, J. Power Sources 196 (2011) 1–12. https://doi.org/10.1016/j.jpowsour.2010.06.084.

[19] C. Brahmi, M. Benltifa, C. Vaulot, L. Michelin, F. Dumur, F. Millange, M. Frigoli, A. Airoudj, F. Morlet-Savary, L. Bousselmi, J. Lalevée, New hybrid MOF/polymer composites for the photodegradation of organic dyes, Eur. Polym. J. 154 (2021). https://doi.org/10.1016/j.eurpolymj.2021.110560.

[20] A.J. Gutie, Flexible PEDOT-nanocellulose composites produced by in situ oxidative polymerization for passive components in frequency filters, (2016) 8062–8067. https://doi.org/10.1007/s10854-016-4804-y.

[21] J. Heinze, Cyclic Voltammetry—"Electrochemical Spectroscopy". New Analytical Methods (25), Angew. Chemie Int. Ed. English 23 (1984) 831–847. https://doi.org/10.1002/anie.198408313.